Contributions of hyperon-hyperon scattering to subthreshold cascade production in heavy ion collisions

Feng Li, Lie-Wen Chen, Che Ming Ko, and Su Houng Lee

Phys. Rev. C **85**, 064902 — Published 6 June 2012

DOI: 10.1103/PhysRevC.85.064902

Contributions of hyperon-hyperon scattering to subthreshold cascade production in heavy ion collisions

Feng Li,[1,*] Lie-Wen Chen,[2,†] Che Ming Ko,[1,‡] and Su Houng Lee[3,§]

[1] *Cyclotron Institute and Department of Physics and Astronomy, Texas A&M University, College Station, TX 77843-3366, USA*

[2] *INPAC, Department of Physics and Shanghai Key Laboratory for Particle Physics and Cosmology, Shanghai Jiao Tong University, Shanghai 200240, China*

[3] *Institute of Physics and Applied Physics, Yonsei University, Seoul 120-749, Korea*

Using a gauged flavor SU(3)-invariant hadronic Lagrangian, we calculate the cross sections for the strangeness-exchange reactions $YY \leftrightarrow N\Xi$ ($Y = \Lambda, \Sigma$) in the Born approximation. These cross sections are then used in the Relativistic Vlasov-Uehling-Uhlenbeck (RVUU) transport model to study Ξ production in Ar+KCl collisions at incident energy of 1.76A GeV and impact parameter $b = 3.5$ fm. We find that including the contributions of hyperon-hyperon scattering channels strongly enhances the yield of Ξ, leading to the abundance ratio $\Xi^-/(\Lambda + \Sigma^0) = 3.38 \times 10^{-3}$, which is essentially consistent with the recently measured value of $(5.6 \pm 1.2^{+1.8}_{-1.7}) \times 10^{-3}$ by the HADES collaboration at GSI.

PACS numbers: 25.75.-q

I. INTRODUCTION

The study of particle production in heavy ion collisions at energies below their thresholds in nucleon-nucleon collisions was a topic of extensive studies during the 1990s [1–5]. The main motivation for such study is that it offers the possibility of extracting information on the nuclear equation of state (EOS) at densities above that of normal nuclear matter. In particular, the yield of strange hadrons, such as the kaon, has been shown to be sensitive to the stiffness of the nuclear equation of state up to three times normal nuclear matter density, with a softer EOS giving a larger yield than a stiff EOS. Indeed, experimental results obtained by the KaoS Collaboration [6] at the Society for Heavy Ion Research (GSI) in Germany on the yield of kaons in heavy ion collisions at subthreshold energies have led to the conclusion that the nuclear equation of state at high densities is soft, consistent with an incompressibility of about 200 MeV extracted from the collective flow studies by the Plastic Ball [7] and EOS [8] Collaborations from Lawrence Berkeley Laboratory (LBL) and the E877 [9] and E895 [10] Collaborations at the Alternating Gradient Synchrotron (AGS) of Brookhaven National Laboratory (BNL). More recently, the doubly strange baryons Ξ from Ar+KCl collisions at 1.76A GeV, which is below the threshold energy of 3.74 GeV in a nucleon-nucleon collision, was measured by the HADES Collaboration at GSI [11]. The measured abundance ratio including the statistical and systematic errors is $\Xi^-/(\Lambda + \Sigma^0) = (5.6 \pm 1.2^{+1.8}_{-1.7}) \times 10^{-3}$. This value is about 10-20 times larger than those given by the statistical model [12] and the relativistic transport model [13]. Because of the very low collision energy, secondary reactions other than the direct reaction $NN \to N\Xi KK$ are expected to contribute significantantly to Ξ production in these collisions. In Ref. [13], the strangeness-exchange reaction $\bar{K}Y \to \pi\Xi$ ($Y = \Lambda, \Sigma$) between antikaon and hyperon was introduced in the Vlasov-Uheling-Uhlenbeck (RVUU) transport model [14] to study Ξ production in heavy ion collisions. The cross sections used in Ref. [13] were taken from the coupled-channel calculation of Ref. [15] based on a gauged flavor SU(3)-invariant hadronic Lagrangian. Since there are more hyperons than anitkaons in heavy ion collisions at this energy, the strangeness-exchange reaction $YY \to N\Xi$ between two hyperons is expected to be important for Ξ production in these collisions. In the present study, we use the same hadronic Lagarangian as in Ref. [15] to evaluate the cross sections for the reaction $YY \to N\Xi$. For an exploratory study, these cross sections are calculated in the Born approximation with the cutoff parameter in the form factors at interaction vertices fitted to the cross sections for the reactions $\bar{K}Y \to \pi\Xi$ obtained in Ref. [15]. For completeness, we also include the reaction $\bar{K}N \to K\Xi$ with its cross section taken from empirically available values. Our results show that the inclusion of the reaction $YY \to N\Xi$ significantly enhances the yield of Ξ in heavy ion collisions at subthreshold energies, resulting in the abundance ratio $\Xi^-/(\Lambda + \Sigma^0) = 3.38 \times 10^{-3}$ in Ar+KCl collisions at 1.76A GeV and impact parameter $b = 3.5$ fm, which is essentially consistent with the recently measured experimental value. We find, however, that the contribution of the reaction $\bar{K}N \to K\Xi$ to the Ξ yield is negligible.

The paper is organized as follows. In Sec. II, we describe the gauged flavor SU(3)-invariant hadronic Lagrangian [15], calculate the amplitudes for the reaction $YY \to N\Xi$ in the Born approximation, and parametrize the resulting cross sections. In Sec. III, we introduce

*Electronic address: lifengphysics@gamil.com
†Electronic address: lwchen@sjtu.edu.cn
‡Electronic address: ko@comp.tamu.edu
§Electronic address: suhoung@yonsei.ac.kr

the parametrization of the empirical cross section for the reaction $\bar{K}N \to K\Xi$ as a function of the center of mass energy. We then briefly review in Sec. IV the RVUU transport model for high energy heavy ion collisions. Numerical results on the time evolution of the Ξ abundance in Ar+KCl collisions at 1.76A GeV and impact parameter $b = 3.5$ fm are presented in Sec. V. Finally, we present some discussions in Sect. VI and a summary in Sec. VII.

II. THE HADRONIC MODEL

Possible reactions for Ξ production from hyperon-hyperon collisions are $\Lambda\Lambda \to N\Xi$, $\Lambda\Sigma \to N\Xi$, and $\Sigma\Sigma \to N\Xi$. Cross sections for these reactions can be evaluated using the same Lagrangian introduced in Ref [15] for studying Ξ production from the reactions $\bar{K}\Lambda \to \pi\Xi$ and $\bar{K}\Sigma \to \pi\Xi$. This Lagrangian is based on the gauged SU(3) flavor symmetry but with empirical masses. The coupling constants are taken, if possible, from empirical information. Otherwise, the SU(3) relations are used to relate unknown coupling constants to known ones. Also, form factors are introduced at interaction vertices to take into account the finite size of hadrons.

A. The Lagrangian

As in Ref. [15], we use the following flavor SU(3)-invariant hadronic Lagrangian for pseudoscalar mesons and baryons

$$\begin{aligned}\mathcal{L} &= i\,\mathtt{Tr}(\bar{B}\not{\partial}B) + \mathtt{Tr}[(\partial_\mu P^\dagger \partial^\mu P)] \\ &+ g'\left\{\mathtt{Tr}\left[(2\alpha-1)\,\bar{B}\gamma^5\gamma^\mu B\partial_\mu P + \bar{B}\gamma^5\gamma^\mu\,(\partial_\mu P)\,B\right]\right\},\end{aligned} \tag{1}$$

where B and P denote, respectively, the baryon and pseudoscalar meson octets

$$B = \begin{pmatrix} \frac{\Sigma^0}{\sqrt{2}} + \frac{\Lambda}{\sqrt{6}} & \Sigma^+ & p \\ \Sigma^- & -\frac{\Sigma^0}{\sqrt{2}} + \frac{\Lambda}{\sqrt{6}} & n \\ -\Xi^- & \Xi^0 & -\sqrt{\frac{2}{3}}\Lambda \end{pmatrix} \tag{2}$$

and

$$P = \frac{1}{\sqrt{2}} \begin{pmatrix} \frac{\pi^0}{\sqrt{2}} + \frac{\eta_8}{\sqrt{6}} + \frac{\eta_1}{\sqrt{3}} & \pi^+ & K^+ \\ \pi^- & -\frac{\pi^0}{\sqrt{2}} + \frac{\eta_8}{\sqrt{6}} + \frac{\eta_1}{\sqrt{3}} & K^0 \\ K^- & \bar{K}^0 & -\sqrt{\frac{2}{3}}\eta_8 + \frac{\eta_1}{\sqrt{3}} \end{pmatrix}, \tag{3}$$

with g' being a coupling constant and α being a parameter.

For the interactions of baryons and pseudoscalar mesons with the vector meson octet V_μ,

$$V = \frac{1}{\sqrt{2}} \begin{pmatrix} \frac{\rho^0}{\sqrt{2}} + \frac{\omega}{\sqrt{2}} & \rho^+ & K^{*+} \\ \rho^- & -\frac{\rho^0}{\sqrt{2}} + \frac{\omega}{\sqrt{2}} & K^{*0} \\ K^{*-} & \bar{K}^{*0} & \phi \end{pmatrix}, \tag{4}$$

they are included by replacing the partial derivative ∂_μ in Eq.(1) with the covariant derivative $D_\mu = \partial_\mu - \frac{i}{2}g\,[V_\mu,]$, where g is another coupling constant.

We further include the tensor interactions between baryons and vector mesons via the interaction Lagrangian

$$\mathcal{L}^t = \frac{g^t}{2m}\mathtt{Tr}\left[(2\alpha-1)\,\bar{B}\sigma^{\mu\nu}B\partial_\mu V_\nu + \bar{B}\sigma^{\mu\nu}\,(\partial_\mu V_\nu)\,B\right], \tag{5}$$

with g^t being the tensor coupling constant.

We note that axial vector mesons such as the $a_1(1260)$ and $K_1(1270)$ are not included in the present study, same as in the very successful boson-exchange model for the nucleon-nucleon and nucleon-hyperon potentials [16, 17]. For scattering between pseudoscalar and vector mesons, axial vector mesons are important, since they appear as s-channel resonances. In meson-baryon and baryon-baryon scattering as considered in the present study, which involve t- and u-channel meson exchanges, the contribution of axial vector mesons is expected to be small compared to that of pseudoscalar and vector mesons as a result their much larger masses.

B. Born approximation to the reactions $\Lambda\Lambda \to N\Xi$, $\Lambda\Sigma \to N\Xi$, and $\Sigma\Sigma \to N\Xi$

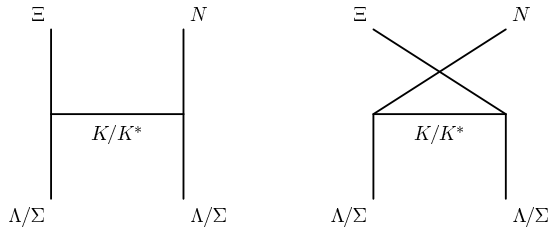

FIG. 1: Born diagrams for the reactions $\Lambda\Lambda \to N\Xi$, $\Lambda\Sigma \to N\Xi$, and $\Sigma\Sigma \to N\Xi$.

In the Born approximation, the reactions $\Lambda\Lambda \to N\Xi$, $\Lambda\Sigma \to N\Xi$, and $\Sigma\Sigma \to N\Xi$ are described by the tree-level t-channel and u-channel diagrams with K and K^* exchanges as shown in Fig. 1. To evaluate their amplitudes requires the following interaction Lagrangian densities that are deduced from the hadronic Lagrangian in the previous subsection, i.e.,

$$\begin{aligned}\mathcal{L}_{KN\Lambda} &= \frac{f_{KN\Lambda}}{m_K}\bar{N}\gamma^5\gamma^\mu\Lambda\partial_\mu K + \text{H.c.}, \\ \mathcal{L}_{KN\Sigma} &= \frac{f_{KN\Sigma}}{m_K}\bar{N}\gamma^5\gamma^\mu(\vec{\tau}\cdot\vec{\Sigma})\partial_\mu K + \text{H.c.}, \\ \mathcal{L}_{K\Lambda\Xi} &= \frac{f_{K\Lambda\Xi}}{m_K}\bar{\Xi}\gamma^5\gamma^\mu\Lambda\partial_\mu K^c + \text{H.c}, \\ \mathcal{L}_{K\Sigma\Xi} &= \frac{f_{K\Sigma\Xi}}{m_K}\bar{\Xi}\gamma^5\gamma^\mu(\vec{\tau}\cdot\vec{\Sigma})\partial_\mu K^c + \text{H.c},\end{aligned}$$

$$
\begin{aligned}
\mathcal{L}_{K^*N\Lambda} &= g_{K^*N\Lambda}\bar{N}\left(\gamma^\mu K^*_\mu + \frac{\kappa_{K^*\Lambda N}}{m_N+m_\Lambda}\sigma^{\mu\nu}\partial_\mu K^*_\nu\right)\Lambda \\
&+ \text{H.c}, \\
\mathcal{L}_{K^*N\Sigma} &= g_{K^*N\Sigma} \\
&\times \vec{\Sigma}\cdot\left(\gamma^\mu\vec{\tau}K^*_\mu + \frac{\kappa_{K^*N\Sigma}}{m_N+m_\Sigma}\sigma^{\mu\nu}\vec{\tau}\partial_\mu K^*_\nu\right)N \\
&+ \text{H.c}, \\
\mathcal{L}_{K^*\Lambda\Xi} &= g_{K^*\Lambda\Xi}\bar{\Xi}\left(\gamma^\mu K^{*c}_\mu + \frac{\kappa_{K^*\Lambda\Xi}}{m_\Lambda+m_\Xi}\sigma^{\mu\nu}\partial_\mu K^{*c}_\nu\right)\Lambda \\
&+ \text{H.c}, \\
\mathcal{L}_{K^*\Sigma\Xi} &= g_{K^*\Sigma\Xi} \\
&\times \vec{\Sigma}\cdot\left(\gamma^\mu\vec{\tau}K^{*c}_\mu + \frac{\kappa_{K^*\Sigma\Xi}}{m_\Sigma+m_\Xi}\sigma^{\mu\nu}\vec{\tau}\partial_\mu K^{*c}_\nu\right)\Xi \\
&+ \text{H.c}.
\end{aligned}
\tag{6}
$$

In the above, $\vec{\tau}$ are Pauli matrices; $\vec{\pi}$, $\vec{\rho}$, and $\vec{\Sigma}$ denote the pion, rho meson, and sigma hyperon isospin triplets, respectively; $K=(K^+,K^0)^T$ ($K^*=(K^{*+},K^{*0})^T$) and $K^c=(\bar{K}^0,-K^-)^T$ ($K^{*c}=(\bar{K}^{*0},-K^{*-})^T$) denote the pseudoscalar (vector) kaon and antikaon isospin doublets, respectively; and $\Xi=(\Xi^0,\Xi^-)^T$ is the cascade hyperon isospin doublet. The coupling constants in above interaction Lagrangian densities are relate to those in Sec. II A by

$$
\begin{aligned}
\frac{f_{KN\Lambda}}{m_K} &= \frac{2\alpha-3}{2\sqrt{3}}g',\ \frac{f_{KN\Sigma}}{m_K} = \frac{2\alpha-1}{2}g', \\
\frac{f_{K\Lambda\Xi}}{m_K} &= \frac{3-4\alpha}{2\sqrt{3}}g',\ \frac{f_{K\Sigma\Xi}}{m_K} = -\frac{1}{2}g', \\
g_{K^*N\Lambda} &= -g_{K^*\Lambda\Xi} = -\frac{\sqrt{3}}{4}g, \\
g_{K^*N\Sigma} &= g_{K^*\Sigma\Xi} = -\frac{g}{4}, \\
\kappa_{K^*\Lambda N} &= \frac{g^t_{K^*\Lambda N}}{g_{K^*\Lambda N}},\ \kappa_{K^*N\Sigma} = \frac{g^t_{K^*N\Sigma}}{g_{K^*N\Sigma}}, \\
\kappa_{K^*\Lambda\Xi} &= \frac{g^t_{K^*\Lambda\Xi}}{g_{K^*\Lambda\Xi}},\ \kappa_{K^*\Sigma\Xi} = \frac{g^t_{K^*\Sigma\Xi}}{g_{K^*\Sigma\Xi}}, \\
\frac{g^t_{K^*N\Lambda}}{m_N+m_\Lambda} &= \frac{2\alpha-3}{2\sqrt{3}}\frac{g^t}{2m},\ \frac{g^t_{K^*N\Sigma}}{m_N+m_\Sigma} = \frac{2\alpha-1}{2}\frac{g^t}{2m}, \\
\frac{g^t_{K^*\Lambda\Xi}}{m_\Lambda+m_\Xi} &= \frac{3-4\alpha}{2\sqrt{3}}\frac{g^t}{2m},\ \frac{g^t_{K^*\Sigma\Xi}}{m_\Sigma+m_\Xi} = -\frac{g^t}{4m}.
\end{aligned}
\tag{7}
$$

The cross sections for these reactions are then given by

$$
\sigma_{YY\to N\Xi}(s) = \frac{1}{64\pi s p_i^2}\int dt\overline{|\mathcal{M}|^2}, \tag{8}
$$

where $s=(p_1+p_2)^2$ and $t=(p_1-p_3)^2$ are the usual squared center of mass energy of colliding hyperons and the squared four momentum transfer in the reaction; and p_i is the momentum of initial hyperons in their center of mass frame. The spin-isospin averaged amplitude $\overline{|\mathcal{M}|^2}$ in the above equation is given by

$$
\begin{aligned}
\overline{|\mathcal{M}|^2} &= \frac{1}{(2s_1+1)(2s_2+1)(2I_1+1)(2I_2+1)} \\
&\times \sum_{s_1s_2s_1's_2'}\Big[\eta_{tt}|\mathcal{M}^t_{s_1s_2s_1's_2'}|^2 - \eta_{tu}\mathcal{M}^t_{s_1s_2s_1's_2'}\mathcal{M}^{u*}_{s_1s_2s_1's_2'} \\
&- \eta_{ut}\mathcal{M}^u_{s_1s_2s_1's_2'}\mathcal{M}^{t*}_{s_1s_2s_1's_2'} + \eta_{uu}|\mathcal{M}^u_{s_1s_2s_1's_2'}|^2\Big],
\end{aligned}
\tag{9}
$$

where $M^t_{s_1s_2s_1's_2'}$ and $M^u_{s_1s_2s_1's_2'}$ are the spin-dependent amplitudes for the two Born diagrams shown in Fig. 1 and are given by

$$
\begin{aligned}
&\mathcal{M}^t_{s_1s_2s_1's_2'}(s,t) = -\frac{f_{KY_1\Xi}f_{KNY_2}}{m_K^2}F^2(\mathbf{p}_1-\mathbf{p}_3,\Lambda) \\
&\times\left[\bar{\Xi}(p_3)\gamma^5\gamma^\mu Y_1(p_1)\right]\frac{t_\mu t_\nu}{t-m_K^2}\left[\bar{N}(p_4)\gamma^5\gamma^\nu Y_2(p_2)\right] \\
&+g_{K^*Y_1\Xi}g_{K^*NY_2} \\
&\times\Bigg[\bar{\Xi}(p_3)\left((1+\kappa_{K^*Y_1\Xi})\gamma^\mu - \kappa_{K^*Y_1\Xi}\frac{(p_3+p_1)^\mu}{m_{Y_1}+m_\Xi}\right) \\
&\times Y_1(p_1)\left]\frac{g_{\mu\nu}-t_\mu t_\nu/m^2_{K^*}}{t-m^2_{K^*}}\left[\bar{N}(p_4)\left((1+\kappa_{K^*NY_2})\gamma^\nu\right.\right.\right. \\
&\left.\left.\left.+\kappa_{K^*NY_2}\frac{(p_3+p_1)^\nu}{m_N+m_{Y_2}}\right)Y_2(p_2)\right]\Bigg]
\end{aligned}
\tag{10}
$$

and

$$
\mathcal{M}^u_{s_1s_2s_1's_2'}(s,u) = \mathcal{M}^t_{s_1s_2s_1's_2'}(s,t), \tag{11}
$$

with $u=(p_1-p_4)^2$. The form factor F introduced at the interaction vertex because of the hardron structure is taken to have the monopole form,

$$
F(\mathbf{q},\Lambda) = \frac{\Lambda^2}{\Lambda^2+\mathbf{q}^2}, \tag{12}
$$

and depends on the three momentum transfer $\mathbf{q}$ and the parameter Λ. The value for Λ depends in general on the meson involved at a vertex. To reduce the number of parameters, we use, however, the same value for Λ at all vertices as in Ref. [15]. The isospin factors η_{tt}, $\eta_{tu}=\eta_{ut}$, and η_{uu} in Eq. (9), which are obtained from summing the isospins of initial and final particle, are 18, 10, and 18 for the reaction $\Sigma\Sigma\to\Xi N$; 6, 2, and 6 for the reaction $\Lambda\Sigma\to\Xi N$, and 2, 2, and 2 for the reaction $\Lambda\Lambda\to\Xi N$.

C. Cross sections for the reactions $\Lambda\Lambda\to N\Xi$, $\Lambda\Sigma\to N\Xi$, and $\Sigma\Sigma\to N\Xi$

For numerical calculations of the cross sections, we use the coupling constants shown in Table I. These values are obtained from $g'=14.4$ GeV^{-1}, $g=13.0$, and $g^t/2m=19.8/m_N$ that are determined from the empirical values $f_{\pi NN}=1.00$, $g_{\rho NN}=3.25$, $g^t_{\rho NN}=19.8$ [18], and $\alpha=0.64$ [19] using relations based on the $SU(3)$ symmetry,

TABLE I: Coupling constants used in the present study.

Vertex	f	Vertex	g	g^t
$KN\Lambda$	-3.52	$K^*N\Lambda$	-5.63	-21.5
$KN\Sigma$	0.992	$K^*N\Sigma$	-3.25	6.31
$K\Lambda\Xi$	0.900	$K^*\Lambda\Xi$	5.63	6.52
$K\Sigma\Xi$	-3.54	$K^*\Sigma\Xi$	-3.25	-26.4

i.e.,

$$\frac{f_{\pi NN}}{m_\pi} = \frac{g'}{2},\ g_{\rho NN} = \frac{g}{4},\ \frac{g^t_{\rho NN}}{2m_N} = \frac{g^t}{4m}. \qquad (13)$$

For the cutoff parameter Λ in the form factor, its value is taken to be $\Lambda = 0.7$ GeV in order to reproduce, as shown in Fig. 2, the cross sections for the reactions $\bar{K}\Lambda \to \pi\Xi$ and $\bar{K}\Sigma \to \pi\Xi$ that are obtained from the coupled-channel calculation based on the same hadronic Lagrangian [15].

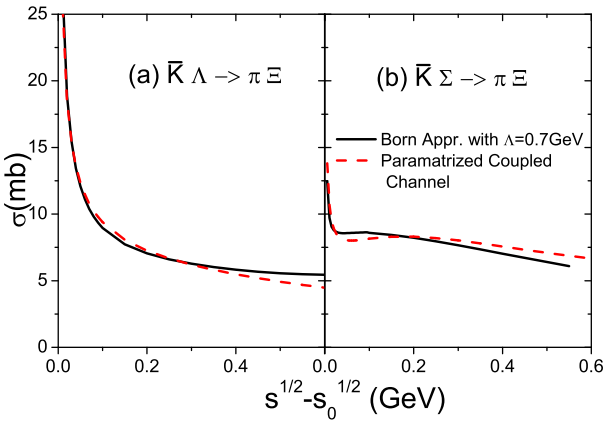

FIG. 2: (Color online) Isospin-averaged cross sections for (a) $\bar{K}\Lambda \to \pi\Xi$ and (b) $\bar{K}\Sigma \to \pi\Xi$. Solid lines are from the Born approximation with the cutoff parameter $\Lambda = 0.7$GeV in the form factor, and dashed lines are those based on the coupled-channel calculation [13, 15].

In Fig. 3, we show by solid lines the isospin-averaged cross sections for the reactions $\Lambda\Lambda \to N\Xi$ (panel (a)), $\Lambda\Sigma \to N\Xi$ (panel (b)), and $\Sigma\Sigma \to N\Xi$ (panel (c)) as functions of the center-of-mass energy $\sqrt{s}$, obtained with $\Lambda = 0.7$ GeV. These cross sections can be parametrized as

$$\begin{aligned}
\sigma_{\Lambda\Lambda\to N\Xi} &= 37.15\frac{p_N}{p_\Lambda}(\sqrt{s}-\sqrt{s_0})^{-0.16}\ \text{mb},\\
\sigma_{\Lambda\Sigma\to N\Xi} &= 25.12(\sqrt{s}-\sqrt{s_0})^{-0.42}\ \text{mb},\\
\sigma_{\Sigma\Sigma\to N\Xi} &= 8.51(\sqrt{s}-\sqrt{s_0})^{-0.395}\ \text{mb}, \qquad (14)
\end{aligned}$$

where p_Λ and p_N are initial Λ and final nucleon momenta in the center-of-mass frame. We note that the magnitude of our cross section for the reaction $\Xi N \to \Lambda\Lambda$ is similar

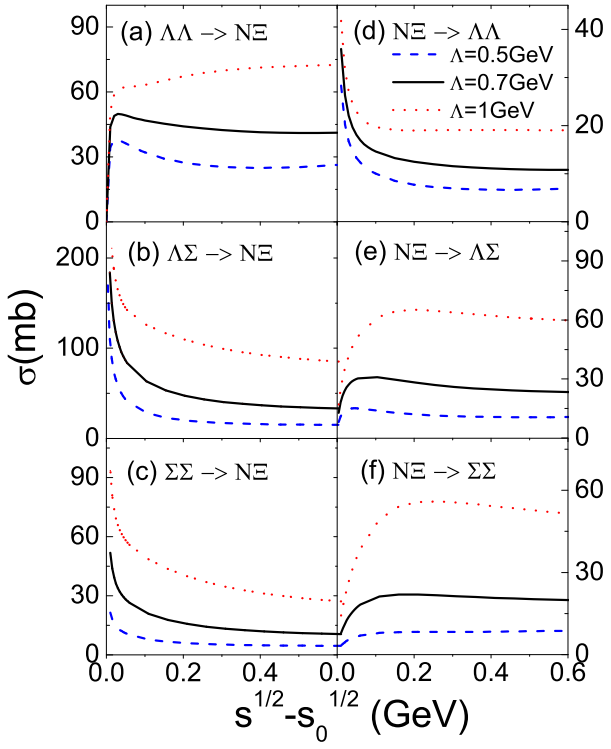

FIG. 3: (Color online) Cross sections for (a) $\Lambda\Lambda \to N\Xi$, (b) $\Lambda\Sigma \to N\Xi$, (c) $\Sigma\Sigma \to N\Xi$, (d) $N\Xi \to \Lambda\Lambda$, (e) $N\Xi \to \Lambda\Sigma$, and (f) $N\Xi \to \Sigma\Sigma$ as functions of the center-of-mass energy $\sqrt{s}$ from the Born approximation with cutoff parameters $\Lambda = 0.5$ GeV (dashed lines), $\Lambda = 0.7$ GeV (solid lines), and $\Lambda = 1$ GeV (dotted lines).

to that of Ref. [20] obtained from the SU_6 quark model formulated in the resonance group method but is smaller than that extracted from the $(K^-, K^+)\Xi^-$ reactions in a nucleus [21]. For comparisons, we also show in Fig. 3 the cross sections for the reaction $YY \to N\Xi$ for the cutoff parameters $\Lambda = 0.5$ GeV (dashed lines) and $\Lambda = 1$ GeV (dotted lines). As expected, the cross sections are larger for a larger Λ.

The cross sections for the inverse reactions $\sigma_{N\Xi\to\Lambda\Lambda}$, $\sigma_{N\Xi\to\Lambda\Sigma}$, and $\sigma_{N\Xi\to\Sigma\Sigma}$ are related to above cross sections by the detailed balance relations:

$$\begin{aligned}
\sigma_{N\Xi\to\Lambda\Lambda} &= \frac{1}{4}\left(\frac{p_\Lambda}{p_N}\right)^2 \sigma_{\Lambda\Lambda\to N\Xi},\\
\sigma_{N\Xi\to\Lambda\Sigma} &= \frac{3}{4}\left(\frac{p_\Lambda}{p_N}\right)^2 \sigma_{\Lambda\Sigma\to N\Xi},\\
\sigma_{N\Xi\to\Sigma\Sigma} &= \frac{9}{4}\left(\frac{p_\Sigma}{p_N}\right)^2 \sigma_{\Sigma\Sigma\to N\Xi}. \qquad (15)
\end{aligned}$$

We note that the cross sections for the reactions $N\Xi \to \Lambda\Lambda$, $\Lambda\Sigma \to N\Xi$, and $\Sigma\Sigma \to N\Xi$ diverge near their threshold energies, since these reactions are exothermic, i.e., the total mass is larger in the initial state than in the final state.

III. CROSS SECTIONS FOR THE REACTION $\bar{K}N \to K\Xi$

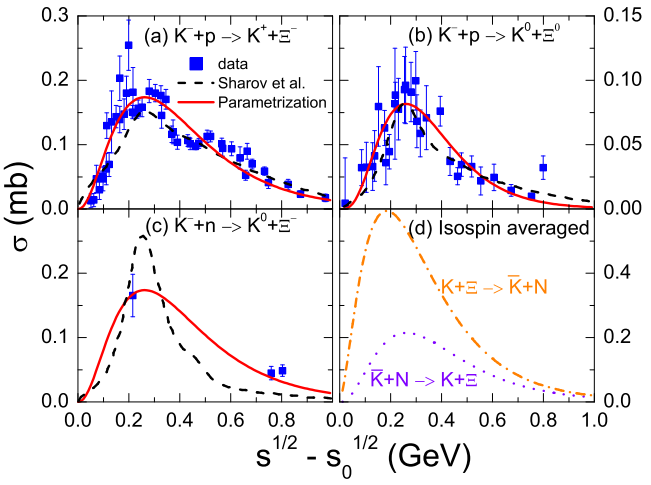

FIG. 4: (Color online) Cross sections for the reaction $K^- + p \to K^+\Xi^-$ (a), $K^-+p \to K^0\Xi^0$ (b), and $K^-+n \to K^0\Xi^0$ (c). Solid squares are experimental data, dashed lines are theoretical results of Ref. [32], and solid lines are our parametrization. Panel (d) shows the isospin averaged cross sections for the reaction $\bar{K}N \to K\Xi$ (dotted line) and its inverse reaction $K\Xi \to \bar{K}N$ (dash-dotted line) based on our parametrization.

For completeness, we also include in the present study the reaction $\bar{K}N \to K\Xi$. Both the differential and total cross sections for this reaction were measured in 1960s and 70s [22–31], and they are shown in Fig. 4 by solid squares for $K^-+p \to K^+\Xi^-$ (panel (a)), $K^-+p \to K^0\Xi^0$ (panel (b)), and $K^- + n \to K^0\Xi^0$ (panel (c)). Recently, a phenomenological model was introduced in Ref. [32] to describe these reactions, and the results are shown by dashed lines in Fig. 4. In the present study, we use the following parametrization for these cross sections:

$$\begin{aligned}
\sigma_{K^-p\to K^+\Xi^-} &= 235.6\left(1-\frac{\sqrt{s_0}}{\sqrt{s}}\right)^{2.4}\left(\frac{\sqrt{s_0}}{\sqrt{s}}\right)^{16.6}\ \text{mb},\\
\sigma_{K^-p\to K^0\Xi^0} &= 7739.9\left(1-\frac{\sqrt{s_0}}{\sqrt{s}}\right)^{3.8}\left(\frac{\sqrt{s_0}}{\sqrt{s}}\right)^{26.5}\ \text{mb},\\
\sigma_{K^-n\to K^0\Xi^-} &= 235.6\left(1-\frac{\sqrt{s_0}}{\sqrt{s}}\right)^{2.4}\left(\frac{\sqrt{s_0}}{\sqrt{s}}\right)^{16.6}\ \text{mb}.
\end{aligned} \tag{16}$$

In terms of these cross sections, the isospin averaged cross section for the reaction $\bar{K}N \to K\Xi$ can be expressed as

$$\begin{aligned}
\sigma_{\bar{K}N\to K\Xi} &= 0.5(\sigma_{K^-p\to K^+\Xi^-} + \sigma_{K^-p\to K^0\Xi^0}\\
&+ \sigma_{K^-n\to K^0\Xi^-}).
\end{aligned} \tag{17}$$

The detailed balance relation then allows us to express the cross section for the inverse reaction $K\Xi \to \bar{K}N$ as

$$\sigma_{K\Xi\to\bar{K}N} = \left(\frac{p_N}{p_\Xi}\right)^2 \sigma_{\bar{K}N\to K\Xi} \tag{18}$$

where p_N and p_Ξ are the 3-momenta of nucleon and Ξ in the center-of-mass frame. In Fig. 4(d), we show the isospin averaged cross section for the reaction $\bar{K}N \to K\Xi$ (dotted line) and its inverse reaction $K\Xi \to \bar{K}N$ (dash-dotted line) based on our parametrization.

IV. THE RELATIVISTIC VLASOV-UHLING-ULENBECK TRANSPORT MODEL

To study Ξ production in heavy ion collisions at subthreshold energies, we generalize the RVUU transport model [14] to include the reactions $YY \to N\Xi$ and $\bar{K}N \to K\Xi$ and their inverse reactions besides the reaction $\bar{K}Y \to \pi\Xi$ and its inverse reaction that were already included in Ref. [13]. In addition to these reactions and other reactions involving nucleons, Delta resonances, hyperons, pions, kaons, and antikaons, the VUU model also includes the mean-field effect on the propagation of baryons, kaons, and antikaons. For nucleons and Delta resonances, their mean-field potentials are taken from the relativistic mean-field model via the scalar and vector potentials, so their motions are given by the following equations of motion:

$$\begin{aligned}
\dot{\mathbf{x}} &= \frac{\mathbf{p}^*}{E^*}\\
\dot{\mathbf{p}} &= -\nabla_x(E^* + W_0)
\end{aligned} \tag{19}$$

where $m^* = m - \Phi$, $\mathbf{p}^* = \mathbf{p} - \mathbf{W}$, $E^* = \sqrt{\mathrm{p}^{*2} + m^{*2}}$ with Φ and $W = (W_0, \mathbf{W})$ being the scalar and vector mean fields, respectively. These mean fields are calculated from the effective chiral Lagrangian of Ref. [33] with parameters determined from fitting the nuclear matter incompressibility $K_0 = 194$MeV and the nucleon effective mass $m^*/m = 0.6$ at normal nuclear matter density $\rho_0 = 0.15$ fm^3. For Λ and Σ hyperons, their mean-field potentials are taken to be 2/3 of the nucleon mean-field potential according to their light quark content. Similarly, the mean-field potential for Ξ is 1/3 of that of the nucleon .

For kaons and antikaons, their mean-field potentials are derived, on the other hand, from the dispersion relation obtained in the chiral Lagrangian [34]

$$\omega_{K,\bar{K}} = \left[m^2_{K,\bar{K}} + \mathbf{p}^2 - \frac{\Sigma_{NK}}{f^2}\rho_s + \left(\frac{3}{8}\frac{\rho_N}{f^2}\right)^2\right]^{1/2} \pm \frac{3}{8}\frac{\rho_N}{f^2}, \tag{20}$$

where $\rho_s = \langle\bar{N}N\rangle$ is the scalar density, $f = 103$ MeV is the pion decay constant, and the $\pm$ is taken as "+" for kaons and "-" for antikaons. The KN and $\bar{K}N$ sigma term Σ_{NK} in the above equation can in principle be calculated from the $SU(3)_L \times SU(3)_R$ chiral Lagrangian but are taken to have the values $\Sigma_{NK}/f^2 = 0.22$ GeV^{2}fm^3 and $\Sigma_{N\bar{K}}/f^2 = 0.35$ GeV^{2}fm^3 as in Ref.[13] from fitting the kaon and antikaon yields in heavy ion collisions.

Besides affecting the propagation of particles, the mean-field potential also has effect on the threshold energy for particle production as a result of the potential difference between the initial and final states of a reaction. For example, this effect is important for understanding the enhanced production of antikaon through the reactions $BB \leftrightarrow BBK\bar{K}$, $\pi B \leftrightarrow K\bar{K}B$, and $\pi Y \leftrightarrow \bar{K}N$ in heavy ion collisions at subthresold energies. As a result, the contribution of the reaction $\bar{K}Y \rightarrow \pi\Xi$ to Ξ production in heavy ion collisions at subthreshold energies was found in Ref. [13] to be further enhanced. We note that in the RVUU model, kaons, antikaons, hyperons (lambdas and sigmas), and cascade particles are treated perturbatively by neglecting the effect of their production and annihilation on the collision dynamics, which is dominated by the more abundant nucleons, Delta resonances, and pions. In this approach, kaons, antikaons, and hyperson are produced from nucleon (Delta)-nucleon (Delta) and pion-nucleon (Delta) collisions whenever it is energetically allowed, and they are given probabilities that are determined by the ratios of their respective production cross sections to the total cross sections of the colliding particles. For Ξ production from antikaon collisions with nucleons or hyperons and from hyperon-hyperon collisions, it is similarly treated but the probability of the produced Ξ is reduced by the probabilities of colliding particles. The annihilation of these rare particles is treated in a similar way and leads to reductions of their probabilities. The present approach thus takes into account the small probability associated with the production of two rare particles in a subthrehold heavy ion collision that are involved in the production of a Ξ.

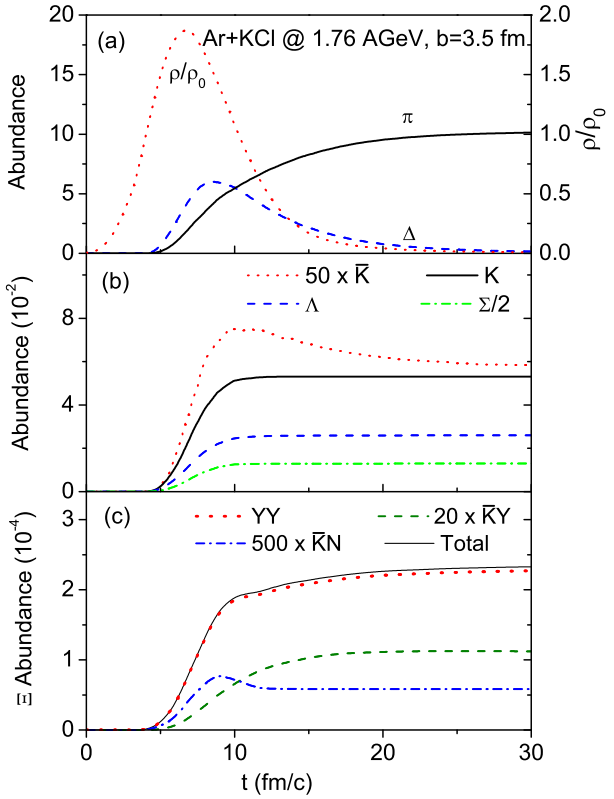

FIG. 5: (Color online) Time evolutions of (a) central baryon density (right scale) and the abundances (left scales) of π, Δ; (b) K, Λ, Σ, and $\bar{K}$; and (c) Ξ produced from different reactions.

V. RESULTS

In this Section, we show the results for ^{40}Ar + KCl collisions at incident energy 1.76 AGeV, taking as an average of $^{40}\mathrm{Ar} + \mathrm{K}^{39}$ collisions and $^{40}\mathrm{Ar} + \mathrm{Cl}^{35}$ collisions, and compare them with the data from the HADES Collaboration at SIS. The HADES trigger (LVL1) selects approximately the most central 35% of the total reaction cross section [11]. According to GEANT simulations [35] with the UrQMD [36, 37] transport approach as event generator, the average value and width of the corresponding impact parameter distribution amount to 3.5 and 1.5 fm, respectively. For simplicity, we take $b = 3.5$ fm in the present study. Fig. 5(a) shows the time evolution of π and Δ abundances (left scale) and the central baryon density (right scale). It is seen that the colliding system reaches its highest density of about $1.87\rho_0$ at about 7 fm/c when most particles are produced. The π abundance saturates at 10.3. Assuming isospin symmetry, the π^- number is then 3.43 which is very close to the measured number of $3.9 \pm 0.1 \pm 0.1$ by the HADES Collaboration [38, 39]. The time evolution for the abundances of K, $\bar{K}$, Λ, and Σ are shown in Fig. 5(b), and they saturate at the values of 5.32×10^{-2}, 1.15×10^{-3}, 2.60×10^{-2}, and 2.60×10^{-2}, respectively. Assuming isospin symmetry gives 2.61×10^{-2} for the K^+ number, 5.75×10^{-4} for the K^- number, and 3.47×10^{-2} for the $\Lambda + \Sigma^0$ number. These numbers are again close to corresponding measured numbers of $(2.8\pm0.2\pm0.1\pm0.1)\times10^{-2}$, $(7.1\pm1.5\pm0.3\pm0.1)\times10^{-4}$, and $(4.09 \pm 0.1 \pm 0.17) \times 10^{-2}$ by the HADES Collaboration [40]. For the time evolution of the Ξ abundance, it is shown by the solid curve in Fig.5(c) and is seen to saturate at the value 2.34×10^{-4}. Taking Ξ^- as half of Ξ by assuming isospin symmetry, we obtained a Ξ^- number of 1.17×10^{-4} which is about half of the measured number of $(2.3 \pm 0.9) \times 10^{-4}$ by the HADES Collaboration [41]. Our results thus lead to an abundance ratio $\Xi^-/(\Lambda + \Sigma^0) = 3.38\times10^{-3}$, which is essentially consistent with the measured value of $(5.6 \pm 1.2^{+1.8}_{-1.7}) \times 10^{-3}$ by the HADES collaboration.

The contributions to Ξ production from different reaction channels are also shown in Fig.5(c). Dotted, dashed-dotted, and dash lines denote, respectively, the abundance of the Ξ particles from the reactions $YY \rightarrow N\Xi$, $\bar{K}Y \rightarrow \pi\Xi$, and $\bar{K}N \rightarrow K\Xi$. Compared to the total Ξ abundance, shown by the solid line in Fig.5, the contributions are 97.5%, 2.40%, and 0.1% from the reactions $YY \rightarrow N\Xi$, $\bar{K}Y \rightarrow \pi\Xi$, and $\bar{K}N \rightarrow K\Xi$, respectively. So the $YY \rightarrow N\Xi$ channel dominates Ξ production in heavy

ion collisions at subthreshold energies. This can be explained by the fact that the cross section for $YY \to N\Xi$ is almost 3-4 times the cross section for $\bar{K}Y \to \pi\Xi$, and almost hundred times the cross section for $\bar{K}N \to K\Xi$. Also, the hyperon abundance in the system is almost 20 times the anti-kaon abundance. We note that the relative contributions to the Ξ yield from the reactions $\Lambda\Lambda \to N\Xi$, $\Lambda\Sigma \to N\Xi$ and $\Sigma\Sigma \to N\Xi$ are about 1, 4 and 1.

VI. DISCUSSIONS

Our results are obtained without the consideration of the isospin asymmetry effect due to different proton and neutron numbers in the colliding nuclei, which is expected to increase the final abundance ratio $\Xi^-/(\Lambda+\Sigma^0)$. If we assume that the abundance of Ξ has reached chemical equilibrium in heavy ion collisions, which is certainly questionable in view of the failure of the statistical model in describing the experimental data, this enhancement can be estimated using $\Xi^-/\Xi^0 = \mathrm{e}^{-\mu_C/T} = \Sigma^-/\Sigma^0 = \Sigma^0/\Sigma^+ = N/Z$, where μ_C is the charge chemical potential and T is the temperature of the system. With the value $N/Z \sim 1.14$ for $\mathrm{Ar}^{40} + \mathrm{K}^{39}$ or $\mathrm{Ar}^{40} + \mathrm{Cl}^{35}$, we have $\Xi^- = 0.533\ \Xi$ and $\Sigma^0 = 0.3314\ \Sigma$, leading to the ratio $\Xi^-/(\Lambda + \Sigma^0) = 3.60 \times 10^{-3}$ that is 6.5% larger than that for an isospin symmetric system.

Also, the nuclear EOS used in the transport model can affect the final Ξ abundance in heavy ion collisions. The results presented in the previous Section are based on a soft EOS. Using a stiff EOS, we find that the Λ, Σ, and Ξ abundances are reduced to 1.74×10^{-2}, 1.77×10^{-2}, and 1.46×10^{-4}, respectively. The reason for this reduction in the hyperon abundances is that the energy density of the colliding system increases faster for a stiff EOS, thus making its expansion faster and reaction time short. However, the abundance ratio $\Xi^-/(\Lambda+\Sigma^0) = 3.13\times10^{-3}$ for the stiff EOS is essentially the same as that for a soft EOS.

Furthermore, the results presented here are for the impact parameter $b = 3.5$ fm. A more realistic comparison with experimental data should include a distribution of impact parameters. We have checked that using different impact parameters, the ratio $\Xi^-/(\Lambda + \Sigma^0)$ remains, however, essentially unchanged, since both hyperons and cascade abundances change by almost the same factor.

Finally, because of the very large Ξ production cross sections and the small size of the colliding system, the geometrical treatment of Ξ production from hyperon-hyperon scattering in terms of their scattering cross section as used in the RVUU transport model may become inaccurate. This can be seen from the dependence of final Ξ abundance on the value of the cutoff parameter Λ in the form factor used in evaluating the cross sections of the reactions $YY \to N\Xi$. As shown in Fig. 3, these cross sections increase with increasing value of Λ. Results from our transport model study show, on the other hand, that the Ξ abundance increases with decreasing value of Λ. However, our conclusion in the present work is expected to remain unchanged since the Ξ abundance changes only by about 30% when the Ξ production cross sections change by more than a factor of 4. We note that a more accurate treatment of particle scattering may be achieved by using the stochastic method of Ref. [42] based on the transition probability, and we hope to purse such an improved study in the future.

VII. SUMMARY

We have calculated the cross sections for the reaction $YY \to N\Xi$ ($Y = \Lambda$, Σ) based on a gauged SU(3)-invariant hadronic Lagrangian in the Born approximation and found that these cross sections are almost 4 times the cross sections for the reaction $\bar{K}Y \to \pi\Xi$ that was considered in previous studies. We then used these cross sections to study Ξ production in ^{40}Ar+KCl collisions at the subthreshold energy of 1.76 AGeV within the frame work of a relativistic transport model that includes explicitly the nucleon, Δ, pion, and perturbatively the kaon, antikaon, hyperons and Ξ. We found that the reaction $YY \to N\Xi$ would enhance the Ξ abundance by a factor of about 16 compared to that from the reaction $\bar{K}Y \to \pi\Xi$, resulting in abundance ratio $\Xi^-/(\Lambda + \Sigma^0) = 3.38 \times 10^{-3}$ that is essentially consistent with that measured by the HADES Collaboration at GSI. Our study has thus helped in resolving one of the puzzles in particle production from heavy ion collisions at subthrehold energies.

Acknowledgements

This work was supported in part by the U.S. National Science Foundation under Grant Nos. PHY-0758115 and PHY-1068572, the Welch Foundation under Grant No. A-1358, the NNSF of China under Grant Nos. 10975097 and 11135011, the Shanghai Rising-Star Program under grant No. 11QH1401100, the "Shu Guang" project supported by Shanghai Municipal Education Commission and Shanghai Education Development Foundation, the Program for Professor of Special Appointment (Eastern Scholar) at Shanghai Institutions of Higher Learning, the Science and Technology Commission of Shanghai Municipality (11DZ2260700), and the Korean Research Foundation under Grant No. KRF-2011-0020333.

[1] J. Aichelin and C.M. Ko, Phys. Rev. Lett. **55**, 2661 (1985).
[2] A. Shor *et al.*, Phys. Rev. Lett. **63**, 2192 (1989).
[3] X.S. Fang, C.M. Ko, G.Q. Li, and Y.M. Zheng, Phys. Rev. C **49**, R608 (1994); Nucl. Phys. A **575**, 766 (1994); G.Q. Li, C.M. Ko, X.S. Fang, and Y.M. Zheng, Phys. Rev. C **49**, 1139 (1994); G.Q. Li, C.M. Ko, and X.S. Fang, Phys. Lett. B **329**, 149 (1994); B.A. Li, C. M. Ko, and G.Q. Li, Phys. Rev. C **50**, R2675 (1994); G.Q. Li and C.M. Ko, Phys. Lett. B **351**, 37 (1995).
[4] U. Mosel, Ann. Rev. Nucl. Part. Sci. **41**, 29 (1992).
[5] S. Teis, W. Cassing, T. Maruyama, and U. Mosel, Phys. Rev. C **50**, 388 (1994).
[6] D. Miskowiec *et al.*, Phys. Rev. Lett. **72**, 3650 (1994); R. Barth *et al.*, *ibid.* **78**, 4007 (1997); F. Laue *et al.*, *ibid.* **82**, 1640 (1999).
[7] H.A. Gustafsson *et al.*, Mod. Phys. Lett. A **3**, 1323 (1988).
[8] M.D. Partlan *et al.*, Phys. Rev. Lett. **75**, 2100 (1995).
[9] J. Barrette *et al.*, Phys. Rev. C **56**, 3254 (1997).
[10] H. Liu *et al.*, Phys. Rev. Lett. **84**, 5488 (2000).
[11] G. Agakishiev *et al.*, Phys. Rev. Lett. **103**, 132301 (2009).
[12] S. Wheaton, J. Cleymans, and M. Hauer, Comput. Phys. Commun. **180**, 84 (2009).
[13] L.W. Chen, C.M. Ko, and Y.Tzeng, Phys. Lett. **B 584**, 269 (2004).
[14] C.M. Ko, Q. Li, and R. Wang, Phys. Rev. Lett. **59** (1987) 1084; C.M. Ko and Q. Li, Phys. Rev. C **37**, 2270 (1988); Q. Li, J.Q. Wu, and C.M. Ko, Phys. Rev. C **39**, 849 (1989); C.M. Ko, Nucl. Phys. A **495**, 321c (1989).
[15] C.H.Li and C.M.Ko, Nucl. Phys. A **712**, 110 (2002).
[16] R. Machleidt, K. Holinde, and C. Elster, Phys. Rept. **149**, 1 (1987).
[17] V.G.J. Stoks, R.A.M. Klomp, C.P.F. Terheggen, and J.J. de Swart, Phys. Rev. C **49**, 2950 (1994).
[18] B. Holzenkamp, K. Holinde, and J. Speth, Nucl. Phys. A **500**, 485 (1989).
[19] R.A. Adelseck and B. Saghai, Phys. Rev. C **42**, 108 (1990).
[20] C. Nakamoto, Y. Fujiwara, and Y. Suzuki, Nucl. Phys. A **639**, 51c (1998).
[21] J.K. Ahn *et al.*, Phys. Lett. B **633**, 214 (2006).
[22] A. de Bellefon *et al.*, Nuovo Cimento A **7**, 567 (1972)
[23] J.P. Berge *et al.*, Phys. Rev. **147**, 945 (1966)
[24] E. Briefel *et al.*, Phys. Rev. D **16**, 2706 (1977)
[25] E. Briefel *et al.*, Phys. Rev. D **12**, 1859 (1975)
[26] G. Burgun *et al.*, Nucl. Phys. B **8**, 447 (1968)
[27] J.R. Charlson, H.F. Davis, *et al.*, Phys. Rev. D **7**, 2533 (1973)
[28] D.D. Carmony, G.M. Pjerrou, and P.E. Schlein, Phys. Rev. Lett. **12**, 482 (1964)
[29] P.M. Dauber *et al.*, Phys. Rev. **179**, 1262 (1969)
[30] J. Griselin et al., Nucl. Phys. B **93**, 189 (1975)
[31] M. Haque, *et al.*, Phys. Rev. **152**, 1148 (1966)
[32] D.A. Sharov, V.L. Krotkikh, and D.E. Lanskoy, Eur. Phys. J. A **47**, 109 (2011).
[33] R.J. Furnstahl, H.B. Tang, and B.D. Serot, Phys. Rev. C **52**, 1368 (1995).
[34] G.Q.Li and C.M.Ko, J. Phys. G: Nucl. Part. **22**, 1673 (1996).
[35] GEANT 3.21, http://consult.cern.ch/writeup/geant/ (1993).
[36] S.A. Bass *et al.*, Prog. Part. Nucl. Phys. **41**, 255 (1998)
[37] M. Bleicher *et al.*, J. Phys. G **25**, 1859 (1999).
[38] G.Agakishiev, *et al.* Eur. Phys. J. A **47**, 63 (2011).
[39] G. Agakishiev *et al.* [HADES Collaboration], Phys. Rev. C **82**, 044907 (2010).
[40] G. Agakishiev *et al.* [HADES Collaboration], Phys. Rev. C **80**, 025209 (2009).
[41] G. Agakishiev *et al.* [HADES Collaboration], Eur. Phys. J. A **47**, 21 (2009).
[42] W. Cassing, Nucl. Phys. A **700**, 618 (2002).